Enantioselective Discrimination via Wireless Chemiresistive Devices

Malinee Niamlaem,[a] Sara Grecchi,[a] Filippo Malacarne,[a] Gerardo Salinas,[b] and Serena Arnaboldi*[a]

Developing chemiresistive devices for the wireless detection of complex analytes has gained considerable interest. In particular, the enantioselective recognition of chiral molecules is still a challenge. Here, we design a hybrid chemiresistive device for the wireless enantioselective discrimination of chiral analytes by combining the enantiorecognition capabilities of an inherently chiral oligomer, that is, oligo-(3,3'-dibenzothiophene) (BT_2T_4) and the insulating/conducting transition of polypyrrole (Ppy). The device is obtained by modifying each extremity of an interdigitated electrode (IDE) with Ppy on the interdigitated area and oligo-BT_2T_4 on the connection pads. Due to the asymmetric electroactivity triggered by bipolar electrochemistry, the wireless enantioselective discrimination of both enantiomers of tryptophan and DOPA was achieved. A difference in the onset resistance values was obtained for both enantiomers due to a favorable or unfavorable diastereomeric interaction between the inherently chiral oligomer and the antipode of the chiral molecule. Interestingly, such a device showed a wide quantification range, from μM to mM levels. This work opens up new alternatives to designing advanced wireless devices in enantiorecognition.

Introduction

Chemiresistive devices are systems where a perturbation on the charge carriers induces changes of resistance (or conductance) due to the presence of a given analyte. These have gained considerable attention[1] since conductivity is a bulk transport property; thus, small perturbations on the mobility of the charge carriers result in significant conductivity changes compared to possible variations in potential or current.[1a,2] Multiple devices based on the insulating/conducting transition of sophisticated carbon-based polymeric materials have been designed to analyze ammonia, methane, cyclohexene, hydrogen sulfide, or hydrogen.[3] Although most chemiresistive sensors proposed in the literature show excellent performance towards a target analyte, preparing the transducing polymeric layer is rather complicated. In addition, these devices require a direct electric connection; hence, developing wireless sensors is still a challenge.

In this context, bipolar electrochemistry (BE) has emerged as an easy and straightforward alternative for the design of wireless transducers of chemical information.[4] BE is based on the asymmetric polarization of a conducting object, or bipolar electrode (BPE), using an external electric field (ε). Under these conditions, a polarization potential difference (ΔV) between the two ends of the BPE is induced. Once the ΔV overcomes the thermodynamic threshold potential (ΔV_{min}), redox reactions occur asymmetrically on each extremity of the conducting object. Such unconventional induction of electroactivity has been used in material science,[5] electrosynthesis[6] and sensing.[7] For example, a wireless chemiresistive device was designed to evaluate the catalytic activity of metallic surfaces towards hydrogen and oxygen evolution reactions. For this, a conducting polymer insulating/conducting transition works as a variable-resistance switch on one extremity of the BPE, whereas water-splitting reactions take place on the opposite side.[8] Such sophisticated approaches open up exciting opportunities for the wireless electroanalysis of more or less complex analytes, e.g., chiral molecules.

As is well known, chirality is one of nature's most important asymmetric features due to its involvement in biology, physics, and chemistry.[9] In particular, developing easy and straightforward approaches for selective enantiorecognition of chiral analytes is of utmost interest. Although multiple enantioselective electrochemical interfaces have been designed,[10] in most of these, chiral recognition is achieved regarding kinetic changes (i.e., current). Recently, inherent chiral oligomers have become a powerful alternative for the efficient differentiation of the antipodes of a chiral molecule.[11] In these π-conjugated materials, enantiorecognition is based on favorable and unfavorable diastereomeric interactions between the chiral oligomeric surface and the enantiomers of a given analyte.[12] Is important to highlight that as it is well-established, in order to induce enantioselectivity, either via diastereomeric interactions or host-guess complexation, a chiral probe and an asymmetric environment are required. Furthermore, the synergy between

[a] Dr. M. Niamlaem, Dr. S. Grecchi, Mr. F. Malacarne, Prof. S. Arnaboldi
Department of Chemistry, Università degli Studi di Milano, Via Golgi 19, 20133 Milano, Italy
E-mail: serena.arnaboldi@unimi.it

[b] Dr. G. Salinas
University of Bordeaux, CNRS, Bordeaux INP, ISM, UMR 5255, F-33607 Pessac, France

the enantioselective capabilities of these materials and BE has been extensively studied for the transduction of chiral information in solution.[13]

In this work, we take advantage of the enantioselective capabilities of 2,2′-bis[2-(5,2′-bithienyl)]3,3′-bithianaphthene (BT_2T_4) and the insulating/conducting transition of polypyrrole (Ppy) to design a hybrid chemiresistive sensor. For this, an interdigitated electrode (IDE), acting as BPE, was modified on one extremity with the oligomers of BT_2T_4 and on the interdigitated part with the charged state of polypyrrole (Ppy^{n+}) (Scheme 1). With such a device, the wireless enantioselective discrimination of the stereoisomers of DOPA and tryptophan as model chiral molecules was carried out. Since enantiorecognition is based on the favorable and unfavorable diastereomeric interactions between the inherent chiral oligomer and the antipode, the resistance of Ppy will change only if the correct enantiomer is present in the solution.

Experimental Section

Pyrrole (99%), D- and L-3,4-dihydroxyphenylalanine (D-, L–DOPA), D-, L- tryptophan (D-, L-Trp) and lithium perchlorate ($LiClO_4$, 99%) were purchased from Sigma Aldrich. Anhydrous acetonitrile (ACN, 99%) was obtained from Honeywell Riedel-de-Haën™. All chemicals were used as received without further purification. The interdigitated electrodes (IDEs, Metrohm) consist of 250 pairs of patterned Au electrodes with a band gap of 5 μm (glass substrate dimensions: Length 2.29 x Width 0.76 x thickness 0.07 cm). Enantiopure inherently chiral oligomer, (S)- or (R)-2,2′-bis[2-(5,2′-bithienyl)]3,3′-bithianaphthene ((S)-BT_2T_4 or (R)-BT_2T_4) was synthesized following a published methodology.[12] Scanning electron microscopy experiments and energy-dispersive X-ray spectroscopy mappings were carried out using a Vega3 Tescan 20.0 kV microscope.

The hybrid bipolar IDEs were prepared following a two-step procedure (Scheme S1a). At first, the electropolymerization of Ppy on IDE (designed as Ppy^{n+}/IDE) was carried out. A two potentiostat system (PGSTAT101, Metrohm Lab Instrument, and a PalmSense4 potentiostat) was connected to a symmetry unit specially designed for the in-situ electrochemical-conductance method.[2,14] In such a setup, an Au IDE (Scheme S1b, left), a platinum (Pt) mesh, and an Ag wire, acting as working, counter, and pseudo-reference electrodes, respectively, were used. The potentiodynamic polymerization was performed on a 0.01 M pyrrole, 0.1 M $LiClO_4$ ACN solution. Briefly, as potentiostat (1) performs the classic potentiodynamic experiment in a potential range between −1.0 V vs. $Ag°$ to 1.3 V vs. $Ag°$, v = 0.1 V/s, and 10 cycles, a constant potential ($\Delta E = 10$ mV) is applied between the branches of the IDE using potentiostat (2) and the symmetry unit (3) (Scheme S1a). The electropolymerization of Ppy was optimized in order to obtain a maximum conductance of
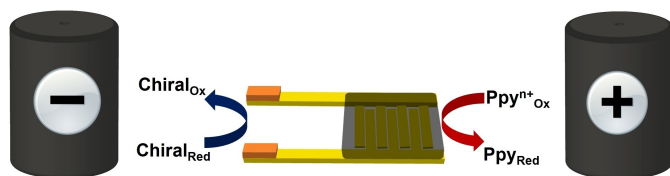
215 mS ± 15 mS. After the interdigitated part was modified, the Ppy^{n+}-coated IDE was used as a working electrode for electro-oligomerizing an enantiopure inherently chiral molecule on the opposite extremity of the IDE (Scheme S1a). The electrosynthesis of the enantiopure oligo-(S)- and oligo-(R)-BT_2T_4 was performed by cyclic voltammetry in a conventional three-electrode cell composed of the Ppy^{n+}/IDE, a Pt wire, and Ag wire, as working, counter and pseudo–reference electrodes, respectively. The potentiodynamic oligomerization was performed by scanning from 0.0 V vs. $Ag°$ to 1.2 V vs. $Ag°$, 0.2 V/s, 36 cycles, in a 0.1 M $LiClO_4$ and 0.75 mM monomer ACN solution. Once again the electro-oligomerization was optimized to obtain a maximum cathodic current of 0.41 mA ± 0.07 mA. After the deposition, the hybrid Ppy^{n+}/IDE/oligo-BT_2T_4 (Scheme S1b, right) device was used as a bipolar electrode for the wireless enantiodiscrimination measurements.

The wireless enantioselective discrimination measurements were carried out in a bipolar cell containing an aqueous 0.2 M $LiClO_4$ solution in the presence of 5 mM L- or D- enantiomer. The antipodes of two different chiral probes were used as model analytes: DOPA and Trp. The hybrid Ppy^{n+}/IDE/oligo-BT_2T_4 (length 2.25 cm) was placed between two graphite feeder electrodes with a separation distance of 5.0 cm, and different electric field values were applied (Scheme S2a). The resistance between the IDE combs was measured ex-situ, after each applied electric field, using a commercial multimeter (Lafayette DMB-1) connected to the Au section of the IDE (Scheme S2b). For the concentration dependence experiments, the range between 0.0001 mM and 10 mM L–DOPA was analyzed with the hybrid Ppy^{n+}/IDE/oligo-(S)-BT_2T_4 at a constant electric field (2.3 V/cm). For the sake of reproducibility all the bipolar experiments were carried out three times.

Results and Discussion

As stated, the hybrid Ppy^{n+}/IDE/oligo-BT_2T_4 device was designed following a two-step procedure. At first, the electro-polymerization of Ppy was carried out using the in-situ electrochemical conductance method. This technique allows us to evaluate the electrical behavior of the polymer during electro-polymerization in real-time.[2] The potentiodynamic polymerization was performed in a 0.01 M pyrrole, 0.1 M $LiClO_4$ ACN solution. As can be seen, the conductance profile exhibits a gradual increase within a potential range between −0.3 and 0.6 V, reaching a maximum value of 215 mS ± 15 mS (Figure S1). According to the principles of the in-situ electrochemical conductance method, as the polymerization progresses, Ppy deposits on the gaps between the interdigits, passing from the insulating region to the percolation and finally to the thin layer. Under the experimental conditions of this work, such transitions occur in the first three potentiodynamic scans. In addition, the electrochemical behavior of the obtained Ppy in a free-monomer 0.1 M $LiClO_4$ ACN solution shows the characteristic asymmetric charge/discharge process of Ppy between −0.6 V vs. $Ag°$ and 0.6 V vs. $Ag°$ (Figure S2). At the same time, the conductance profile exhibits a sigmoidal response where the insulating/conducting transitions occur between −0.3 V vs. $Ag°$ and −0.9 V vs. $Ag°$ (Figure S2). The conductance profile's hysteresis ($\Delta E_G \approx 0.6$ V) is characteristic of the rather slow insulating/conducting transition of π-conjugated polymers.[15]

Scheme 1. Schematic illustration of the BE experiment for enantioselective discrimination on the hybrid IDE bipolar electrode, representing the redox reactions occurring on both sides of the BPE. The orange, black, and yellow parts stand for the oligo-BT_2T_4, the Ppy^{n+}, and the Au branches, respectively.

After this, the electro-oligomerization of the inherently chiral monomer on the opposite extremity of the IDE was carried out. This work used 2,2'-bis[2-(5,2'-bithienyl)]3,3'-bithia-naphthene, BT_2T_4, as an inherent chiral monomer due to its outstanding enantioselective capabilities.[11,13b,16] Figure S3 shows the cyclic voltammograms obtained during the oligome-rization of both enantiomers of BT_2T_4, taking place on the opposite extremity of the Ppy^{n+}/IDE in a 0.75 mM monomer, 0.1 M of $LiClO_4$ ACN solution (36 cycles). As it is established, the oxidation of BT_2T_4 shows, in the first cycle, two oxidation peaks characteristic of the bithianaphthene core and the thiophene moiety. However, the gradual increase of the anodic and cathodic current at lower potentials than the oxidation of the monomer demonstrates the surface modification of the pads of the IDE. SEM analysis coupled with EDX spectroscopy was carried out to confirm each polymeric successful deposition. Three regions have been examined: the Ppy^{n+}/IDE part, the pristine Au, and the Au/oligo-BT_2T_4 section. The SEM images present three well-defined morphologies: a globular surface of Ppy on top of the Au interdigits and between the gaps, a relatively smooth surface for the pristine Au, and a granular morphology for the oligo-BT_2T_4 (Figure 1a–c). The EDX signal for

the Ppy^{n+}/IDE section shows the presence of carbon (C–Kα), nitrogen (N–Kα), and gold (Au–Kα), in comparison with the pristine Au section (Au–Kα) (Figure 1d, black and yellow lines), evidencing the presence of Ppy on the interdigitated structure. On the contrary, the oligo-BT_2T_4 section shows the characteristic signals of sulfur (S–Kα), accompanied by an increase of the carbon signal (C–Kα), corroborating the deposit of the inherent chiral oligomer (Figure 1d, orange line).

After the fabrication and characterization of the hybrid bipolar electrode, the wireless enantiorecognition was tested. As the first proof-of-concept, the two enantiomers of DOPA were used as chiral analytes. For this, two independent Ppy^{n+}/IDE/oligo-(S)-BT_2T_4 devices were placed separately at the center of a bipolar cell containing an aqueous 0.2 M $LiClO_4$ solution in the presence of 5 mM L- or D-DOPA. Under these conditions, redox reactions are induced at the extremities of the BPE when a high enough electric field is applied. Thus, the oxidation of the chiral analyte triggers an electron flow from the anodic to the cathodic extremity of the BPE, resulting in the reduction of Ppy^{n+}. In particular, such reduction causes a change in the doping state of this conjugated polymer, leading to variations in its resistance; hence, Ppy acts as a variable-resistance switch. As it can be seen, by using the device functionalized with the oligo-(S) (Figures 2a and S4) and in the presence of L–DOPA or D-DOPA at low electric field values ($\varepsilon <$ below 1.5 V/cm), there is not enough driving force to induce the redox reactions. Thus, the resistance of Ppy remains almost unchanged. However, above this threshold ε, the redox reactions occur, causing a considerable increase in the resistance. As expected, when using the oligo-(S) BPE, such transition occurs above 1.5 V/cm in the presence of L–DOPA and around 3.0 V/cm for D-DOPA (Figures 2a and S4). This indicates that the hybrid Ppy^{n+}/IDE/oligo-(S)-BT_2T_4 preferably reacts with L–DOPA, reflected by a rather large onset electric field separation ($\Delta\varepsilon_{onset}$) of 1.5 V/cm. Such a clear separation between the resistance profile obtained for the two enantiomers is associated with the favorable or unfavorable diastereomeric interactions between the inherently chiral oligomeric film and the two antipodes of DOPA in solution.

As it is well-established by classic electrochemistry, a peak-to-peak separation between the two enantiomers of DOPA of around 200 mV and 300 mV has been obtained when using electrodes modified with inherent chiral oligomers.[11b,13a] Thus, in a first-order approximation, such thermodynamic difference is directly translated to a shift of the threshold electric field in BE. The specular result was obtained using the Ppy^{n+}/IDE/oligo-(R)-BT_2T_4 BPE (Figure 2b). Once again, threshold electric field values of 1.5 V/cm for D-DOPA and 3.0 V/cm for L–DOPA were obtained when using an oligo-(R) device. Thus, the oligo-(R) BPE reacts preferentially with D-DOPA due to the favorable diaster-eomeric interactions. This agrees with the enantiorecognition of DOPA performed with classic electrochemistry (Figure S5) and with alternative bipolar systems based on actuation, rotation, and light emission.[13] Furthermore, these results demonstrate the possible use of π-conjugated polymers as variable-resist-ance switches to transduce chiral information in solution.
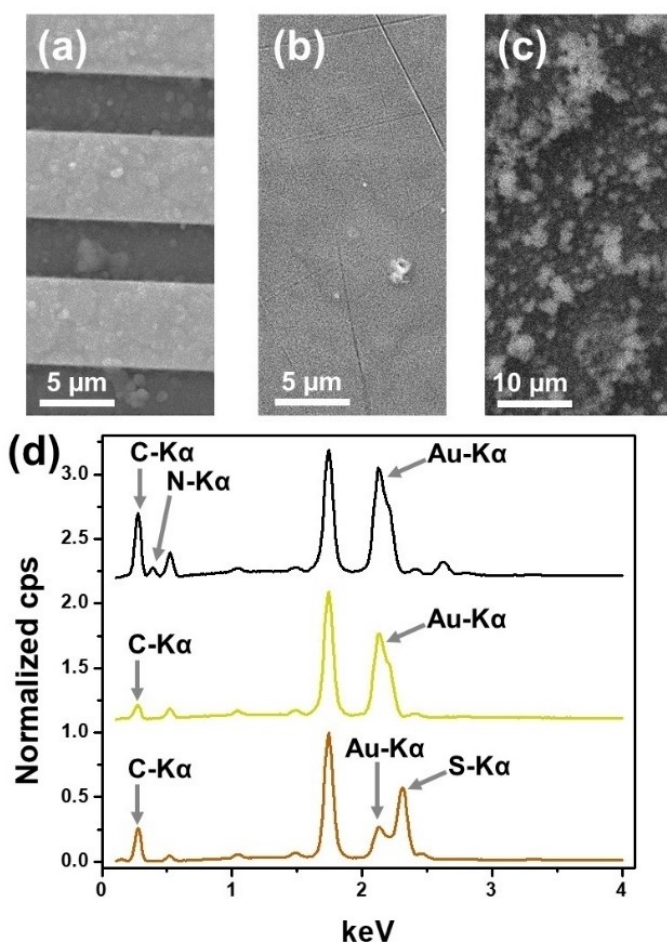

Figure 1. SEM images of (a) the Ppy^{n+}/IDE, (b) pristine Au, and (c) Au/oligo-BT_2T_4 surfaces. (d) EDX signals for measuring the emission peak of carbon, nitrogen, gold, and sulfur at the surface of the Ppy^{n+}/IDE (black line), pristine Au (yellow line), and Au/oligo-BT_2T_4 (orange line) sections.

ChemPlusChem

Research Article
doi.org/10.1002/cplu.202400310

Chemistry Europe
European Chemical
Societies Publishing

hybrid chemiresistive BPE, we evaluate the possible quantitative analysis of chiral molecules in solution in the next step. The resistance was measured as a function of L–DOPA concentration, ranging from 0.1 μM to 10 mM. In this case, a constant electric field of 2.3 V/cm was applied across a bipolar cell containing a hybrid Ppy^{n+}/IDE/oligo-(S)-BT_2T_4 device. The resistance plot as a function of L–DOPA concentrations exhibits a linear correlation ($R^2 = 0.983$) (Figure 2c). Interestingly, resistance changes were obtained even at extremely low concentrations of L–DOPA (0.1 μM). As stated above, small perturbations on the mobility of the charge carriers result in significant conductivity changes since conductivity is a bulk transport property. Such an outstanding range of quantification demonstrates the efficiency of resistance as a physicochemical readout of chemical information, in comparison with current and potential in conventional electrochemistry, or bending, rotation and light emission in bipolar electrochemistry measurements.

Finally, the possible analysis of alternative chiral analytes has been explored to verify the approach's general validity. The resistance profile as a function of the applied electric field was evaluated in the presence of both tryptophan enantiomers (Trp). In this case, two independent Ppy^{n+}/IDE/oligo-(S)-BT_2T_4 devices were placed separately in a bipolar cell containing an aqueous 0.2 M $LiClO_4$ solution in the presence either of 5 mM L- or D-Trp. Once again, no resistance changes were observed under these conditions at electric field values below 2 V/cm for both enantiomers (Figures 3 and S6). However, the conducting/insulating transition for the oligo-(S) device occurs around 2.1 V/cm for D-Trp and 3.0 V/cm for L-Trp (Figures 3 and S6). However, the $\Delta\varepsilon_{onset}$ is similar to that obtained for the enantiomers of DOPA; the opposite diastereomeric interaction was observed for Trp. Hence, a favorable interaction was
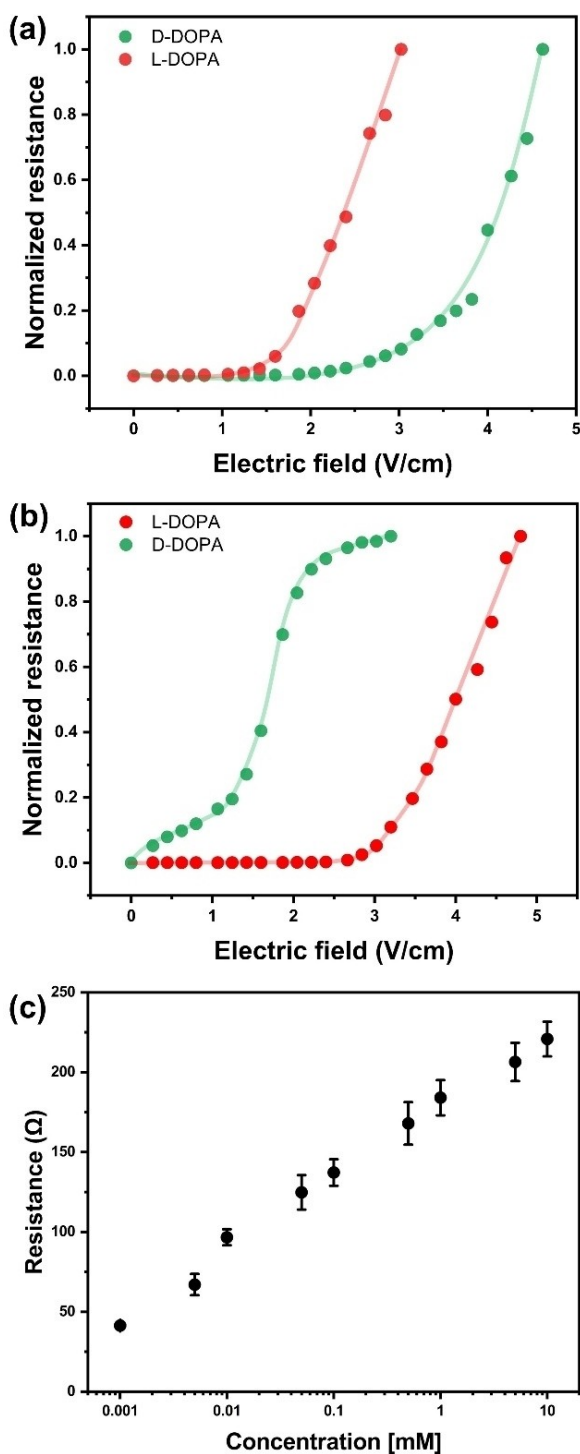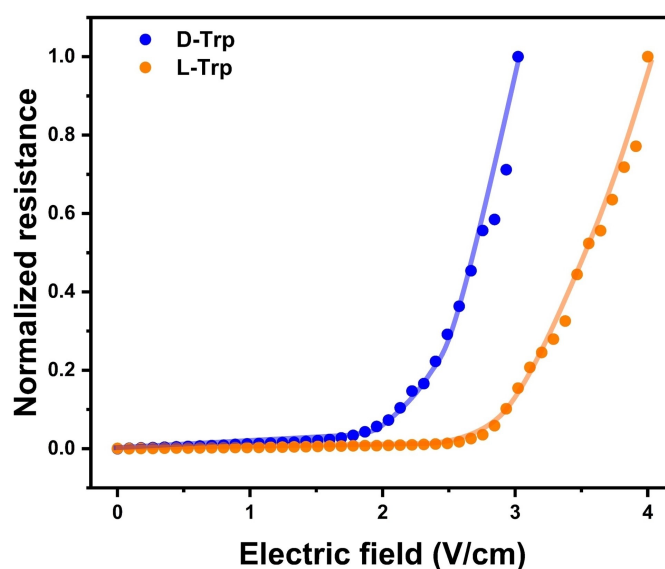
Figure 2. Normalized resistance plots as a function of the applied electric field for the enantioselective discrimination of the antipodes of DOPA using (a) a hybrid Ppy^{n+}/IDE/oligo-(S)-BT_2T_4 and (b) a hybrid Ppy^{n+}/IDE/oligo-(R)-BT_2T_4 bipolar electrodes obtained in a 5 mM DOPA, 0.2 M $LiClO_4$ aqueous solution. (c) Resistance as a function of L–DOPA concentration obtained in a 0.2 M $LiClO_4$ aqueous solution using a hybrid Ppy^{n+}/IDE/oligo-(S)-BT_2T_4 device with a constant applied electric field of 2.3 V/cm. The readout time for all bipolar experiments was 5 s and the error bars represent the average of three measurements.

After this set of experiments corroborating the wireless enantioselective recognition of chiral analytes utilizing the

Figure 3. Normalized resistance plot as a function of the applied electric field for the enantioselective discrimination of the antipodes of Trp (indicated in the figure) using a hybrid Ppy^{n+}/IDE/oligo-(S)-BT_2T_4 bipolar electrode, obtained in a 5 mM Trp, 0.2 M $LiClO_4$ aqueous solution. The readout time for all bipolar experiments was 5 s.

RIGHTS LINK

ChemPlusChem

Research Article
doi.org/10.1002/cplu.202400310

Chemistry Europe
European Chemical
Societies Publishing

obtained, leading to a lower threshold electric field between the oligo-(S)-BT_2T_4 and D-Trp.

In contrast, the opposite occurred in the presence of the L-antipode because of the unfavorable diastereomeric interaction. This was corroborated by using the Ppy^{n+}/IDE/oligo-(R)-BT_2T_4 in the presence of D-Trp, where the conducting/insulating transition takes place at 3.6 V/cm. Thus, an unfavorable interaction occurs (Figure S7). These results illustrate the possible use of wireless chemiresistive-based bipolar electrodes as analytical tools for enantiorecognition of different electroactive chiral analytes.

Conclusions

In conclusion, a hybrid chemiresistive device based on interdigitated electrodes was designed for the wireless enantio-selective discrimination of chiral probes in solution. The bipolar electrode consists of an IDE modified on each of its extremities with Ppy on the interdigitated section and oligo-BT_2T_4 on the connection pads. This device takes advantage of the asymmetric electroactivity generated by bipolar electrochemistry. For this, the enantiorecognition occurs on the inherently chiral oligomer, where the differentiation is based on favorable and unfavorable diastereomeric interactions, and the transduction of information appears on the Ppy extremity, which acts as a variable-resistance switch. As a result, the onset resistance values differed for both enantiomers of DOPA and Trp, which were used as model chiral analytes. Furthermore, the resistance is directly proportional to the chiral analyte concentration in an outstanding range of quantification (from μM to mM) surpassing the performance of alternative bipolar systems. Finally, the presented simple approach can be considered a complementary tool to alternative enantiorecognition techniques, i.e., spectroscopic methods. Thus, this proof-of-concept work paves the way for the design of advanced wireless devices in enantioselective discrimination.

Supporting Information Summary

Supplementary Information (SI) is available including experimental procedures of the in-situ electrochemical-conductance method, electropolymerization on the IDE, schematic illustration of the BE experiment, additional enantiomeric detection measurements, and potentiodynamic study.

Conflict of Interests

The authors declare no conflict of interest.

Data Availability Statement

The data that support the findings of this study are available from the corresponding author upon reasonable request.

[1] a) T. M. Swager, *Macromolecules* **2017**, *50*, 4867–4886; b) W.-T. Koo, J.-S. Jang, I.-D. Kim, *Chem* **2019**, *5*, 1938–1963; c) H. Zhang, Z. Zhang, Z. Li, H. Han, W. Song, J. Yi, *Nat. Commun.* **2023**, *14*, 3495; d) V. Schroeder, E. D. Evans, Y.-C. M. Wu, C.-C. A. Voll, B. R. McDonald, S. Savagatrup, T. M. Swager, *ACS Sens.* **2019**, *4*, 2101–2108; e) S.-X. L. Luo, T. M. Swager, *Nat. Rev. Methods Primers* **2023**, *3*, 73.

[2] G. Salinas, B. A. Frontana-Uribe, *ChemElectroChem* **2019**, *6*, 4105–4117.

[3] a) R.-Q. Lu, S.-X. L. Luo, Q. He, A. Concellón, T. M. Swager, *Adv. Funct. Mater.* **2021**, *31*, 2007281; b) B. Yoon, S.-J. Choi, T. M. Swager, G. F. Walsh, *ACS Sens.* **2021**, *6*, 3056–3062; c) M. J. Bezdek, S.-X. L. Luo, R. Y. Liu, Q. He, T. M. Swager, *ACS Cent. Sci.* **2021**, *7*, 1572–1580; d) S.-X. L. Luo, W. Yuan, M. Xue, H. Feng, M. J. Bezdek, T. Palacios, T. M. Swager, *ACS Nano* **2023**, *17*, 2679–2688; e) T. Zhang, H. Qi, Z. Liao, Y. D. Horev, L. A. Panes-Ruiz, P. S. Petkov, Z. Zhang, R. Shivhare, P. Zhang, K. Liu, V. Bezugly, S. Liu, Z. Zheng, S. Mannsfeld, T. Heine, G. Cuniberti, H. Haick, E. Zschech, U. Kaiser, R. Dong, X. Feng, *Nat. Commun.* **2019**, *10*, 4225; f) W.-T. Koo, H.-J. Cho, D.-H. Kim, Y. H. Kim, H. Shin, R. M. Penner, I.-D. Kim, *ACS Nano* **2020**, *14*, 14284–14322; g) Y. C. Wong, B. C. Ang, A. S. M. A. Haseeb, A. A. Baharuddin, Y. H. Wong, *J. Electrochem. Soc.* **2020**, *167*, 037503.

[4] a) S. E. Fosdick, K. N. Knust, K. Scida, R. M. Crooks, *Angew. Chem. Int. Ed.* **2013**, *52*, 10438–10456; b) N. Shida, Y. Zhou, S. Inagi, *Acc. Chem. Res.* **2019**, *52*, 2598–2608; c) G. Loget, D. Zigah, L. Bouffier, N. Sojic, A. Kuhn, *Acc. Chem. Res.* **2013**, *46*, 2513–2523; d) C. A. C. Sequeira, D. S. P. Cardoso, M. L. F. Gameiro, *Chem. Eng. Commun.* **2016**, *203*, 1001–1008; e) K. L. Rahn, R. K. Anand, *Anal. Chem.* **2021**, *93*, 103–123.

[5] a) G. Loget, J. Roche, E. Gianessi, L. Bouffier, A. Kuhn, *J. Am. Chem. Soc.* **2012**, *134*, 20033–20036; b) O. Phuakkong, M. Sentic, H. Li, C. Warakulwit, J. Limtrakul, N. Sojic, A. Kuhn, V. Ravaine, D. Zigah, *Langmuir* **2016**, *32*, 12995–13002; c) M. Niamlaem, O. Phuakkong, P. Garrigue, B. Goudeau, V. Ravaine, A. Kuhn, C. Warakulwit, D. Zigah, *ACS Appl. Mater. Interfaces* **2020**, *12*, 23378–23387.

[6] a) N. Shida, S. Inagi, *Chem. Commun.* **2020**, *56*, 14327–14336; b) S. Inagi, Y. Ishiguro, M. Atobe, T. Fuchigami, *Angew. Chem. Int. Ed.* **2010**, *49*, 10136–10139.

[7] R. K. Anand, E. S. Johnson, D. T. Chiu, *J. Am. Chem. Soc.* **2015**, *137*, 776–783.

[8] T. Nicolini, Y. Boukarkour, S. Reculusa, N. Sojic, A. Kuhn, G. Salinas, *Electrochim. Acta* **2023**, *458*, 142506.

[9] a) E. Naghdi, R. Ahmadloo, M. Shadi, G. E. Moran, *Trends Environ. Anal. Chem.* **2023**, *40*, e00219; b) C. Zhou, S. Yuan, W. Zhao, W. Guo, H. Ren, *RSC Adv.* **2022**, *12*, 22131–22138; c) A. Kousar, J. Liu, N. Mehwish, F. Wang, A. Y. Dang-i, C. Feng, *Mater. Today Chem.* **2019**, *11*, 217–224.

[10] a) W. Gong, Z. Chen, J. Dong, Y. Liu, Y. Cui, *Chem. Rev.* **2022**, *122*, 9078–9144; b) N. Shukla, A. J. Gellman, *Nat. Mater.* **2020**, *19*, 939–945; c) C. Wattanakit, *Curr. Opin. Electrochem.* **2018**, *7*, 54–60; d) W. Qi, C. Ma, Y. Yan, J. Huang, *Curr. Opin. Colloid Interface Sci.* **2021**, *56*, 101526; e) X. Niu, X. Yang, H. Li, J. Liu, Z. Liu, K. Wang, *Microchim. Acta* **2020**, *187*, 676; f) X. Wei, Y. Chen, S. He, H. Lian, X. Cao, B. Liu, *Electrochim. Acta* **2021**, *400*, 139464; g) J. C. Lang, D. W. Armstrong, *Curr. Opin. Colloid Interface Sci.* **2017**, *32*, 94–107.

[11] a) S. Arnaboldi, S. Grecchi, M. Magni, P. Mussini, *Curr. Opin. Electrochem.* **2018**, *7*, 188–199; b) S. Arnaboldi, T. Benincori, R. Cirilli, S. Grecchi, L. Santagostini, F. Sannicolò, P. R. Mussini, *Anal. Bioanal. Chem.* **2016**, *408*, 7243–7254.

ChemPlusChem

Research Article
doi.org/10.1002/cplu.202400310

Chemistry Europe
European Chemical
Societies Publishing

[12] F. Sannicolò, S. Arnaboldi, T. Benincori, V. Bonometti, R. Cirilli, L. Dunsch, W. Kutner, G. Longhi, P. R. Mussini, M. Panigati, M. Pierini, S. Rizzo, *Angew. Chem. Int. Ed.* **2014**, *53*, 2623–2627.

[13] a) S. Arnaboldi, G. Salinas, G. Bonetti, R. Cirilli, T. Benincori, A. Kuhn, *ACS Meas. Sci. Au* **2021**, *1*, 110–116; b) S. Arnaboldi, B. Gupta, T. Benincori, G. Bonetti, R. Cirilli, A. Kuhn, *Chem. Mater.* **2020**, *32*, 10663–10669; c) S. Arnaboldi, B. Gupta, T. Benincori, G. Bonetti, R. Cirilli, A. Kuhn, *Anal. Chem.* **2020**, *92*, 10042–10047; d) G. Salinas, G. Bonetti, R. Cirilli, T. Benincori, A. Kuhn, S. Arnaboldi, *Electrochim. Acta* **2022**, *421*, 140494; e) S. Arnaboldi, G. Salinas, G. Bonetti, R. Cirilli, T. Benincori, A. Kuhn, *Biosens. Bioelectron.* **2022**, *218*, 114740.

[14] K. Murugappan, M. R. Castell, *Electrochem. Commun.* **2018**, *87*, 40–43.

[15] a) T. Nicolini, A. V. Marquez, B. Goudeau, A. Kuhn, G. Salinas, *J. Phys. Chem. Lett.* **2021**, *12*, 10422–10428; b) A. G. Porras-Gutiérrez, B. A. Frontana-Uribe, S. Gutiérrez-Granados, S. Griveau, F. Bedioui, *Electrochim. Acta* **2013**, *89*, 840–847; c) H. J. Ahonen, J. Lukkari, J. Kankare, *Macromolecules* **2000**, *33*, 6787–6793; d) M. Erginer, E. Sezer, B. Ustamehmetoğlu, J. Heinze, *Electrochim. Acta* **2012**, *67*, 181–186.

[16] S. Arnaboldi, D. Vigo, M. Longhi, F. Orsini, S. Riva, S. Grecchi, E. Giacovelli, V. Guglielmi, R. Cirilli, G. Longhi, G. Mazzeo, T. Benincori, P. R. Mussini, *ChemElectroChem* **2019**, *6*, 4204–4214.

RESEARCH ARTICLE
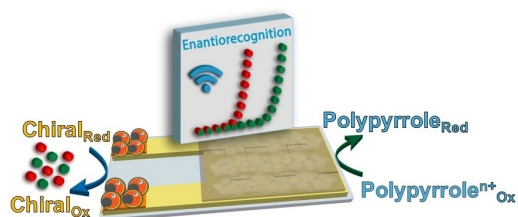
Dr. M. Niamlaem, Dr. S. Grecchi, Mr. F. Malacarne, Dr. G. Salinas, Prof. S. Arnaboldi*

Enantioselective Discrimination via Wireless Chemiresistive Devices

The wireless enantioselective discrimination of tryptophan and DOPA on a hybrid $Ppy^{n+}/IDE/oligo-BT_2T_4$ bipolar electrode was investigated using bipolar electrochemistry. Results revealed that a difference in the onset resistance values was achieved guided by an inherently chiral oligomer and an insulating/conducting polymer.